Thermochimica Acta, 37 (1980) 1—30

THERMAL HAZARD EVALUATION BY AN ACCELERATING RATE CALORIMETER

D.I. TOWNSEND

Process and Development Laboratories, The Dow Chemical Company, Midland, MI 48640 (U.S.A.)

and J.C. TOU

Analytical Laboratories, The Dow Chemical Company, Midland, MI 48640 (U.S.A.)

(Received 29 May 1979)

ABSTRACT

An accelerating rate calorimeter was developed for thermal hazard evaluation to provide time—temperature—pressure data for chemical reactions taking place under adiabatic conditions. The data interpretation is illustrated with an *n*th-order reaction. An approximate analytical solution for the time-to-maximum-rate is formulated, and its accuracy and utility are discussed. The technique was applied to a study of the thermal decomposition of *N*-methyl-*N*-nitroso-*p*-toluene sulfonamide, commonly known as Diazald®, and a complex runaway reaction taking place in a monomer system.

NOTATION

k	rate constant
k^*	pseudo rate constant
A	frequency factor
E	activation energy
n	order of reaction
C_0	initial concentration
C	concentration at time t
M	mass of sample
$\overline{C}_v$	average heat capacity
T_0	initial temperature
T	temperature at time t
T_f	final temperature
T_m	temperature at maximum rate
ΔT_{AB}	adiabatic temperature rise
H_r	heat of reaction
m_0	self-heat rate at T_0
m_T	self-heat rate at T
m_m	self-heat rate at T_m
θ_m	time to maximum rate at temperature T
θ_{m_0}	time to maximum at temperature T_0

Same notations with subscript s are used for the entire system comprising of the sample and the sample bomb, such as $T_{0,s}$, $T_{f,s}$, $T_{m,s}$, $\Delta T_{AB,s}$, $m_{0,s}$, $m_{T,s}$, $m_{m,s}$, $0_{m,s}$, $0_{m0,s}$.

T^* minimum initial temperature above which only the deceleration of the reaction is taking place

T_{NR} temperature of no return

U heat transfer coefficient

a surface area available for heat transfer

T_E temperature of the heat exchanger

$\theta_{T_{NR}}$ time to maximum rate at T_{NR}

ϕ thermal inertia

M_b mass of the bomb

$C_{v,b}$ average heat capacity of the bomb

INTRODUCTION

Because of their impact on the safety of manufacturing, transporting, storage, and processing a chemical, hazard evaluations are extremely important and involve areas of study in which chemistry and engineering come together in an attempt to describe the factors causing, influencing, and preventing an undesirable event. One of the hazards of most concern in the chemical industry is the thermal hazard, which is governed by the thermodynamics and chemical kinetics of the usually complex chemical reactions taking place in the chemical system.

The following two relevant questions concerning temperature and pressure are always encountered before any preventive measures can be taken.

(1) Is there an exothermic reaction taking place? If there is, how much and how fast, and in what temperature range is the heat of reaction released?

(2) Is there any pressure build-up in the system? If there is, how much and how fast, and in what temperature range is the pressure build-up in the reaction? The crucial question is whether the pressure build-up will cause a rupture of the vessel containing the chemicals.

Many techniques have been developed to pursue the answer to the above questions.

Differential scanning calorimetry (DSC) or quantitative differential thermal analysis are the most commonly used techniques, in which not only the heat of reaction but also the reaction kinetics can be evaluated [1]. Recently, a technique based on Ozawa's kinetic treatment [2] was proposed to ASTM committee E-27 on hazard potential of chemicals as an ASTM standard method [3]. However, in thermal hazard evaluation, reactions with releasing gaseous products are very often encountered. The standard commercial aluminum sample pans cannot withstand the pressure build-up, so the rupture of the sample pans during the experiment makes the quantitative evaluation of the DSC data very difficult.

In order to resolve the draw-back, several high pressure sample containers were developed; they are sealed stainless steel cells [4], sealed glass capillary tube sample holders [5,6], Teflon® sealed metal cells [7—9], adhesive

bonded aluminum pans [10], flat base flint glass ampules [11], sealed glass ampule microreactors [12], and the commercial Perkin—Elmer O-ring sealed stainless steel pans. However, sample holders containing polymeric materials are not suitable for routine hazard evaluation because of temperature limitations. A modified sealed glass ampule microreactor [13] with less thermal lagging than that previously reported [12] was used successfully and routinely for thermal hazard evaluation up to 500°C in our laboratory.

A sensitive exothermic reaction detector [14], on the principle of dynamic differential thermal analysis, was developed with a sensitivity of about 1 W kg^{-1} as compared to that of DSC with a sensitivity of 20 W kg^{-1}. All the techniques described above offer information to define temperature and/or the heat of reaction of an exothermic reaction. However, no information concerning pressure was obtained by use of these methods.

An isothermal screening device [15] has been reported, which records both the differential temperature—time and pressure—time responses at different isothermal temperatures. The data obtained are qualitative and mainly for screening purposes. A large-scale test method was recently proposed to the ASTM E-27 committee for determining the self-accelerating decomposition temperature or SADT. The test is performed on samples in commercial packages and the SADT is used to determine conditions for safe storage and transportation. The method was originally proposed for organic peroxides. Before utilization of this large-scale test as a general technique for thermal hazard evaluation, environmental consideration should be given.

Recently, two new techniques [16,17], both based on the adiabatic calorimetric principle, were developed specifically for thermal kinetic hazard evaluations. With these techniques not only can the kinetic aspects of temperature and pressure associated with chemical reactions be evaluated, but also the heat of reaction can be determined. In this paper, the general principle of an accelerating rate calorimeter, one of the two new techniques mentioned above, is described. Examples are also given to illustrate the utility of the technique in the field of hazard evaluations.

EXPERIMENTAL

The accelerating rate calorimeter (ARC) was initially developed in the laboratories of the Dow Chemical Company. Recently, Columbia Scientific Industries of Austin, Texas, added a microprocessor control and commercialized the unit under an abbreviated name CSI—ARC. The basic principle of the ARC is quite simple. It involves maintaining a sample in an adiabatic condition once an exothermic reaction is detected. The heat generated from the reaction will accelerate the reaction. However, an instrumental execution of this adiabatic requirement is a challenging technological problem.

A detailed description of the commercial CSI—ARC can be found elsewhere [18]. A brief discussion of the instrumental design and the operational logic follows.

As shown in Fig. 1, a spherical sample bomb is mounted inside a nickel plated copper jacket with a swagelok fitting to a 1/16 in. tee, on which is

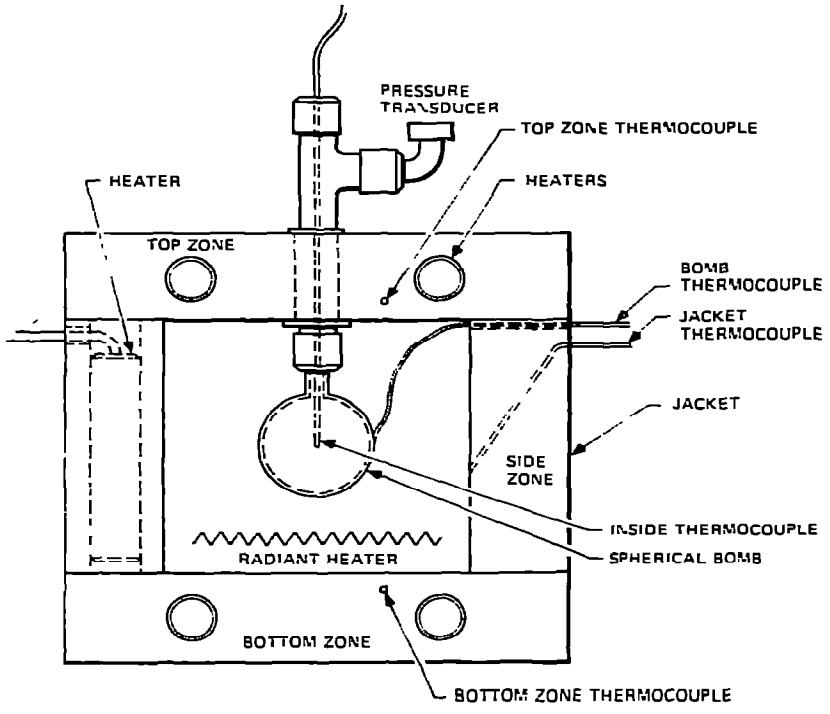

Fig. 1. An accelerating rate calorimeter.

attached a pressure transducer and a sample thermocouple. The jacket is composed of three zones, top, side, and base, which are individually heated and controlled by the Nisil/Nicrosil type N thermocouples. The thermocouples are cemented on the inside surface of the jacket at a point one-quarter the distance between the two cartridge heaters. The point is half-way between the hottest and coldest spots of the jacket. The same type of thermocouple is clamped directly on the outside surface of the spherical sample bomb. All the thermocouples are referenced to the ice point which is designed to be stable to within 0.01°C. Adiabatic conditions are achieved by maintaining the bomb and jacket temperatures exactly equal. However, a slightly mismatched thermocouple attached to the bomb and jacket can cause a drift from adiabaticity, and therefore must be corrected. The drift corrections are performed normally every 50°C for the entire temperature range by applying the required offset voltage. The corrections at any other temperature are obtained by interpolation. With these corrections or calibrations the system will maintain its adiabaticity at any temperature. During an exothermic reaction, the temperature differences between the bomb and three zones of the jacket are digitally controlled to maintain zero by employing commonly used proportional, differential, and integral control algorithms until the completion of the reaction.

The pressure of the reaction system is monitored with a Sersotec 0—2500 psi TJE pressure transducer. In order to protect the transducer from overpressure damage, a chemiquip pressure limiting valve is installed to automatically shut-off the transducer when the pressure increases beyond 2500 psi. For

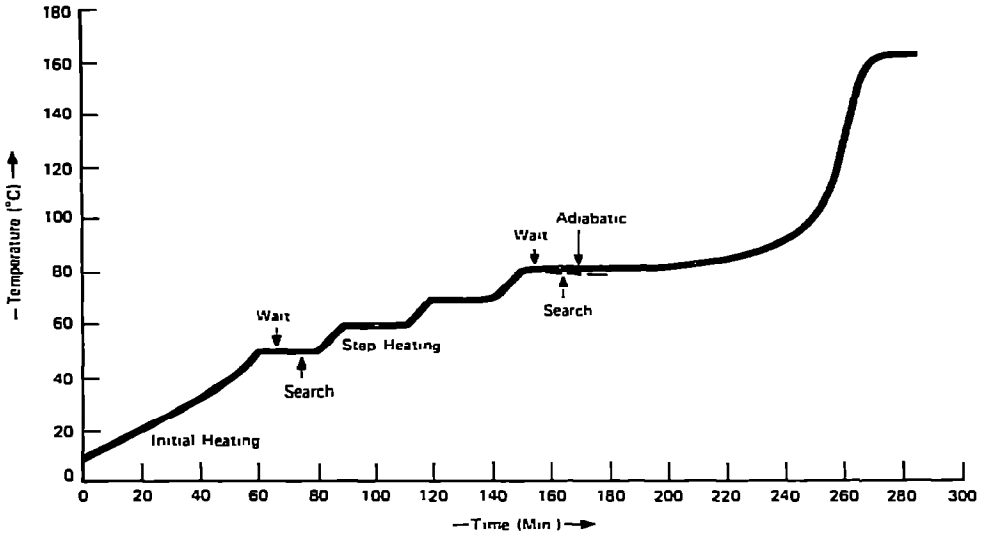

Fig. 2. The heat—wait—search operation mode of an accelerating rate calorimeter.

safety precaution, the entire calorimeter in an insulated aluminum canister is mounted inside a rugged steel contaminant vessel.

The heat—wait—search operational logic of the ARC is shown in Fig. 2. The ARC is first heated to a desired starting temperature and held a period of time for thermal equilibrium to be achieved before a rate search is performed. If the rate is less than the preset rate, the ARC will proceed automatically to the preselected temperature step heat—wait—search sequence until a self-heat rate greater than the preset rate is detected. The calorimeter will be maintained at adiabatic conditions until the completion of the experiment. The stepwise heating is accomplished with a radiant heater located at the bottom of the jacket as shown in Fig. 1. The performance of a CSI—ARC was characterized by Pate and Solem [19], with the decomposition of di-*t*-butyl peroxide in a heavy weight Hastelloy C bomb ~70 g. The precision of the kinetic data was determined from 16 runs with a sample load of ~2 g, which gives a thermal inertia, $\phi \sim 7.0$. The results are summarized in Table 1. For a kinetic event the precision is very satisfactory; the accuracy is very difficult to evaluate. The literature values for the activation energy of decomposition of di-*t*-butyl peroxide are all obtained at isothermal conditions and in different types of solvents. They are 38.0 kcal mol^{-1} in *t*-butyl benzene [20], 36.0 kcal mol^{-1} in toluene [21], 34.0 kcal mol^{-1} [21] and 39.1 kcal mol^{-1} [23] in the vapor phase, 37.5 kcal mol^{-1} in *i*-propylbenzene, 38.0 kcal mol^{-1} in *t*-butylbenzene, and 37.0 kcal mol^{-1} in tri-*n*-butylamine [23]. The ARC value found is lower than the literature values, excluding the case of vapor phase study. In order to evaluate the solvent effect, a 14.6 weight-% di-*t*-butyl-peroxide in mineral oil was re-run in the CSI—ARC. The activation energy was found to be 38.9 kcal mol^{-1}. The above comparison presents an overall estimation of the accuracy of the ARC for a kinetic determination.

In the study of the thermal decomposition of Diazald, 1.01 g of Diazald

TABLE 1

The precision * of the thermokinetic parameters obtained from a CSI—ARC for di-*t*-butyl peroxide

	Mean ($\overline{X}$)	Standard deviation (σ)	Relative precision [($\sigma/\overline{X}$) × 100%]
Adiabatic temperature rise, ΔT_{AB}	67.6°C	± 5.2°C	± 7.7%
Frequency factor, A (in ln unit)	35.20	± 1.02	± 2.9%
Activation energy, E	36.11 kcal mol^{-1}	± 0.82 kcal mol^{-1}	± 2.3%
Reaction order, n	0.925	± 0.088	± 9.5%

* Evaluated from 16 runs.

and 2.88 g of diethyl ether were loaded in a bomb weighing 19.39 g and having a volume of 9 cm^3. This gives a calculated thermal inertia, $\phi = 2.0$, assuming heat capacities of the sample and Hasteloy C as 0.5 cal °C-g^{-1} and 0.1 cal °C-g^{-1}, respectively. The starting temperature and the calorimetric detection sensitivity were set at 50°C and 0.02°C min^{-1}, respectively. After the calorimeter reached 50°C, the 5°C heat—10 min wait—search was carried out automatically by the microprocessor control until a rate greater than 0.02°C min^{-1} was detected. The calorimeter was than maintained at adiabatic conditions until the completion of the reaction. The heat of decomposition of the same Diazald solution was also determined with a modified sealed glass ampule microreactor [13] utilizing a DuPont DSC unit driven by a DuPont 990 programmer. The temperature scanning rate was 10°C min^{-1} with nitrogen flow at a rate 50 cm^3 min^{-1}.

The ARC study of the thermal runaway reaction of a monomer sample was carried out under the same conditions as those of the Diazald solution experiment.

GENERAL PRINCIPLE

In the study of temperature effect on the rate constants of a chemical reaction, it is well recognized that the rate constants of the reaction increase exponentially with temperature. This is demonstrated in the following classical Arrhenius equation

$$k = Ae^{-E/RT} \tag{1}$$

where k is the rate constant of the reaction at temperature T, A is the frequency factor, E is the activation energy of the reaction, and R is the gas constant.

For an nth-order reaction with a single reactant, the rate of the reaction is

$$\frac{dC}{dt} = -kC^n \tag{2}$$

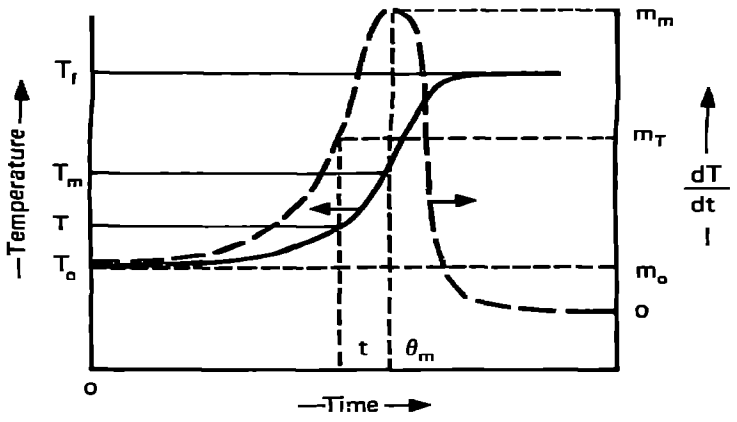

Fig. 3. The temperature and self-heat rate vs. time curves of an adiabatic reaction.

where C is the concentration of the reactant at time t. For an exothermic reaction at adiabatic conditions, the heat generated from the reaction at an initial temperature T_0 will result in a temperature rise, which in turn accelerates the rate of the reaction as shown in eqns. (1) and (2). However, associated with the acceleration of the rate is the depletion of the concentration of the reactant. Therefore, the rate of the reaction is expected to decrease after reaching its maximum value at temperature T_m and finally diminishes to zero at the completion of the reaction at temperature T_f. The expected temperature vs. time curve for an adiabatic reaction system is shown in Fig. 3. At any temperature T or time t, the concentration of the reactant can be approximately related to the temperature of the system

$$C = \frac{T_f - T}{\Delta T_{AB}} C_0 \tag{3a}$$

where ΔT_{AB} is the adiabatic temperature rise, $T_f - T_0$, and C_0 the initial concentration of the reactant. The heat of reaction, ΔH_r, can therefore be calculated from

$$\Delta H_r = M\overline{C}_v \Delta T_{AB} \tag{4}$$

if the average heat capacity, $\overline{C}_v$, over the experimental temperature range and the mass of the sample, M, are known.

Substituting eqn. (3a) after differentiation with respect to T, into eqn. (2) leads to the following fundamental equation relating the thermal measurable quality, T, to a kinetic event

$$m_T = \frac{dT}{dt} = k\left(\frac{T_f - T}{\Delta T_{AB}}\right)^n \Delta T_{AB} C_0^{n-1} \tag{5}$$

where m_T is called the self-heat rate measured at temperature T, or time t.

Rearranging eqn. (5), we have

$$k^* = C_0^{n-1} k = \frac{m_T}{\left(\frac{T_f - T}{\Delta T_{AB}}\right)^n \Delta T_{AB}} \tag{6a}$$

where k^* is a pseudo zero-order rate constant at temperature T. Substituting eqn. (1) into eqn. (6), one obtains

$$\ln k^* = \ln C_0^{n-1} A - \frac{E}{R}\left(\frac{1}{T}\right) \tag{6b}$$

The plot of $\ln k^*$ vs. $1/T$ is, therefore, expected to be a straight line providing the order of reaction is correctly chosen. This is of diagnostic importance. The Arrhenius kinetic parameters, E and A, can be calculated from the plot accordingly.

The temperature, T_m, at the maximum self-heat rate, m_m can be obtained when evaluated at

$$\frac{d^2T}{dt^2} = 0, \text{ i.e.}$$

$$nRT_m^2 + ET_m - ET_f = 0 \tag{7a}$$

or

$$T_m = \frac{E}{2nR}\left(\sqrt{1 + \frac{4nRT_f}{E}} - 1\right) \tag{7b}$$

The self-heat rate, m_T, at any temperature T is given by

$$m_T = m_0\left(\frac{T_f - T}{\Delta T_{AB}}\right)^n e^{\frac{E}{R}\left(\frac{1}{T_0} - \frac{1}{T}\right)} \tag{8}$$

where m_0 is the initial self-heat rate at temperature T_0. When the reaction just begins, the concentration of the reaction has not changed significantly from the initial value, C_0, and eqn. (5) reduces to

$$m_0 = k\Delta T_{AB} C_0^{n-1} \tag{9a}$$

or

$$\ln m_0 = \ln \Delta T_{AB} C_0^{n-1} A - \frac{E}{R}\left(\frac{1}{T_0}\right) \tag{9b}$$

The plot of the initial self-heat rate against the reciprocal of the initial temperature will yield a straight line with a slope $-E/R$; this is called a zero-order line.

As the initial temperature increases, the initial self-heat rate increases following the zero-order line. One very interesting phenomenon occurs when the maximum self-heat coincides with the initial self-heat rate. Above this temperature, the reaction decelerates, even though the temperature itself continues to increase. This temperature is designated as T^* and can be evaluated according to eqn. (7a), when $T_m = T_0 = T^*$ and $T_f = \Delta T_{AB} + T^*$

$$T^* = \sqrt{\frac{E\Delta T_{AB}}{nR}} \tag{10}$$

providing that there is no mechanistic change in the temperature range of interest.

This equation indicates that, theoretically, there always exist a tempera-

ture, T^*, for a reaction, above which the concentration depletion effect on the reaction rate is more drastic than the acceleration effect due to the temperature rise. This phenomenon can take place not only in a pure chemical system, but also in a system with thermal inertia, ϕ, which will lower the adiabatic temperature rise, ΔT_{AB}. The concept of thermal inertia will be discussed later.

Time to maximum rate (TMR)

The self-heat rates of an nth-order reaction have been shown in eqn. (5). It is also important to know the temperature—time relationship, which is an integrated form of eqn. (5).

The upper boundary of the integration is set at the temperature of the maximum self-heat rate. The mathematical significance of this choice is that the boundary, expressed in terms of the intrinsic kinetic parameters as shown in eqn. (7a), does not involve any ill-defined physical parameters, such as the strength of a vessel, the pressure of the system. Physically, the time to maximum self-heat rate may or may not indicate the time to an actually physical destruction.

For a reaction with high activities energy, for example, $E > 20\,000$ cal mol^{-1}, the major portion of reaction time is the TMR. Above T_m, the reaction decelerates rather quickly until the completion of the reaction.

By applying this boundary condition, the integrated form of eqn. (5) becomes

$$\theta_m = t_m - t = \int_t^{t_m} dt = \int_T^{T_m} \frac{dT}{k\left(\frac{T_f - T}{\Delta T_{AB}}\right)^n \Delta T_{AB} C_0^{n-1}} \tag{11}$$

where t_m is the time at T_m, and θ_m is the TMR. This equation can be integrated numerically. However, an approximate analytical solution can also be achieved from the following argument.

Many rate equations have been proposed with a general form of

$$k = \alpha T^j e^{-E/RT}$$

where $j = 0$, Arrhenius equation; 0.5, collision theory; 1, absolute rate theory. The low-order temperature effect in the pre-exponential factor is overshadowed by the widely varying exponential factor itself. For an easy manipulation of the integration of eqn. (11) j was kept as a floating integer.

In demonstrating the present approach, a second-order reaction is utilized as an illustrative example. The self-heat rate expressed in eqn. (5) can be written as

$$m_T = k(T_f^2 - 2TT_f + T^2)C_0 \Delta T_{AB} \tag{12}$$

By keeping j as a floating integer, the above equation can be expressed as follows after making a substitution for the rate constant

$$m_T = (\alpha_1 T_f^2 - 2\alpha_2 T_f + \alpha_3) T^2 e^{-E/RT} C_0 \Delta T_{AB} \tag{13}$$

which is in a readily integratable form. After integration, we have

$$\theta_m = \frac{-1}{C_0 \Delta T_{AB}(\alpha_1 T_f^2 - 2\alpha_2 T_f + \alpha_3)} \frac{R}{E\, e^{-E/RT}} \Bigg|_T^{T_m} = \frac{-RT^2}{m_T E} \Bigg|_T^{T_m}$$

or

$$\theta_m = \frac{RT^2}{m_T E} - \frac{RT_m^2}{m_m E} \tag{14}$$

Based on the same argument and mathematical operations, the same equation can be obtained for other nth-order reactions.

Equation (14) is, therefore, a general approximate analytical solution of the TMR. The plot of θ_m against T^2/m_T is a straight line with slope R/E and intercept $-RT_m^2/M_m E$.

For a reaction with a high activation energy, as will be discussed later, the second term is relatively insignificant as compared to the first term. Then

$$\theta_m \simeq \frac{RT^2}{m_T E} \tag{15}$$

This is equivalent to the equation derived for the determination of homogeneous condensed explosives following a first-order rate reaction [25,26]. By substituting the self-heat rate, eqn. (5), into the above equation, the following expression can be obtained

$$\ln \theta_m = \ln \frac{RT^2}{C_0^{n-1}\left(\frac{T_f - T}{\Delta T_{AB}}\right)^n \Delta T_{AB} E} - \ln A + \frac{E}{R}\left(\frac{1}{T}\right) \tag{16}$$

It was found that the second term, $\ln A$, is significantly greater than the first term over a wide temperature range of a reaction with high activation energy, or

$$\ln \theta_m \simeq \frac{E}{R}\left(\frac{1}{T}\right) - \ln A$$

i.e.

$$\ln \theta_m \simeq -\ln k \text{ or } \theta_m \simeq 1/k \tag{17}$$

Again, this is the equation for a straight line from which the activation energy can be estimated.

A family of such curves starting at different initial temperatures T_0 can also be described by an equation similar to eqn. (17).

$$\ln \theta_{m_0} \simeq \frac{E}{R}\left(\frac{1}{T_0}\right) - \ln A \tag{18}$$

This is the TMR vs. temperature curve for a zero-order reaction. Since the two equations are under different approximation conditions, the activation energies estimated from two equations are slightly different.

Temperature of no return (T_{NR})

The zero-order TMR vs. temperature relationship has its importance in estimating the temperature of no return, T_{NR}, for a reaction vessel with a

known heat transfer property. Below T_{NR}, the reaction temperature will never increase, since all reaction heat can be transferred from the system. Above T_{NR}, the reaction temperature will spiral upward and a runaway reaction will result.

The temperature of no return, T_{NR}, can be determined under the balance of the following two heat-rate equations:

(1) the initial heat release rate from the chemical system at an initial temperature T_0 is

$$M\bar{C}_v A\, e^{-E/RT_0}\, \Delta T_{AB} C_0^{n-1} \tag{19}$$

(2) the heat transfer rate from the chemical system to the heat exchanger at temperature T_E is

$$Ua(T_0 - T_E) \tag{20}$$

where U is the overall heat transfer coefficient, and a the heat transfer area.

At thermal equilibrium, the heat release rate equals the heat transfer rate, i.e.

$$M\bar{C}_v A\, e^{-E/RT_0}\, \Delta T_{AB} C_0^{n-1} = Ua(T_0 - T_E) \tag{21}$$

As shown in Fig. 4, when $T_0 < T_{NR}$ there are two numerical solutions to the equation. No runaway reaction is expected to take place when the temperatures of the chemical system and the heat exchanger are below T_0' and at T_E, respectively. However, as T_0 increases to T_{NR}, only one solution is possible. At this point, the slope of the heat generation line equals that of the heat transfer line, or

$$M\bar{C}_v A\, e^{-E/RT_0} \left(\frac{E}{RT_0^2}\right) \Delta T_{AB} C_0^{n-1}\Big|_{T_0 = T_{NR}} = Ua \tag{22}$$

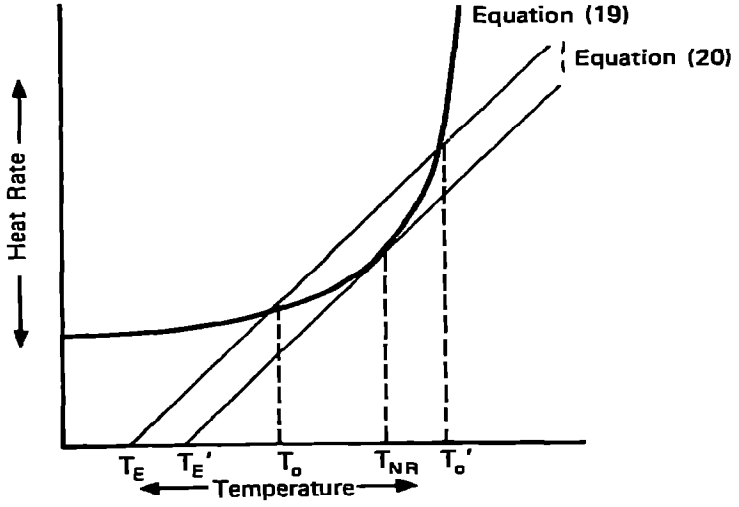

Fig. 4. The self-heat rate and heat transfer rate vs. temperature curves.

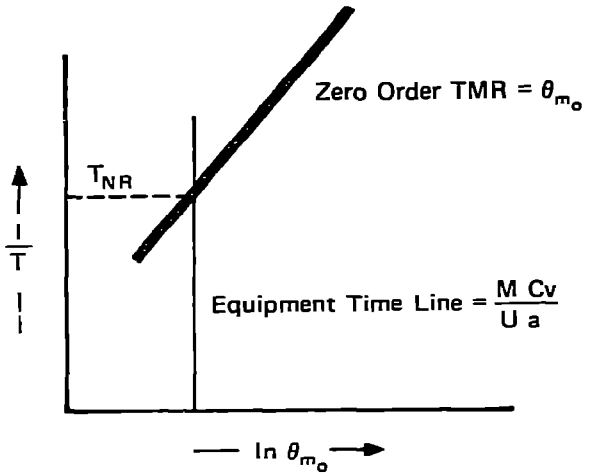

Fig. 5. The graphical determination of T_{NR}.

in which case

$$\frac{RT_0^2}{C_0^{n-1}\Delta T_{AB}A\ e^{-E/RT_0}E} = \theta_{m_0}$$

then

$$\theta_{m_0} \text{ at } T_{NR} \text{ or } \theta_{T_{NR}} = \frac{MC_v}{Ua} \tag{23}$$

The quantity, MC_v/Ua, represents the time line for the equipment, and the quantity, $\theta_{T_{NR}}$, is the adiabatic zero-order time to maximum rate at T_{NR}. Therefore, T_{NR} can be graphically determined from the intersection of the above two lines, as shown in Fig. 5.

Thermal inertia (ϕ)

All the equations described above have been developed for a sample held at adiabatic conditions in the sense that all the generated energy has gone into simply heating the chemical system. In the present accelerating rate calorimetric system, part of the heat generated from the reaction is being used to heat up the sample bomb as well. Thermodynamically, the following heat balance can be written

$$M\overline{C}_v\Delta T_{AB} = (M\overline{C}_v + M_b\overline{C}_{vb})\Delta T_{AB,s}$$

where M_b and $\overline{C}_{vb}$ are the mass and the heat capacity of the bomb and $\Delta T_{AB,s}$ the adiabatic temperature rise for the total system comprising the sample and the sample bomb. Therefore

$$\Delta T_{AB} = \phi\Delta T_{AB,s} \tag{24}$$

where

$$\phi = 1 + M_b\overline{C}_{vb}/M\overline{C}_v$$

The quantity, ϕ, is called thermal inertia. The inverse of thermal inertia, $1/\phi$ is commonly understood to be the degree of adiabaticity.

The temperature rise of the sample, ΔT_{AB}, and the heat of reaction can then be calculated from $\Delta T_{AB,s}$ determined experimentally by use of eqns. (24) and (4). The adiabatic final temperature of the sample, T_f, is thus

$$T_f = T_0 + \phi \Delta T_{AB,s} \tag{25}$$

providing there is no mechanism change over the temperature range. For the kinetic treatment of experimental data, identical operations as discussed previously are applicable. The two fundamental eqns. (3) and (5) now become

$$C = \frac{T_{f,s} - T}{\Delta T_{AB,s}} C_0 \tag{3b}$$

and

$$m_{T,S} = k \left(\frac{T_{f,s} - T}{\Delta T_{AB,s}} \right)^n \Delta T_{AB,s} C_0^{n-1}$$

where the subscripts reflect that the measurement is made for the system.

The pseudo zero-order rate constants, k^*, and therefore the fundamental kinetic parameters, A and E, can be evaluated in an identical manner to the calculations based on isolated chemicals ($\phi = 1$).

Once the kinetic, A and E, and thermodynamic, ΔT_{AB} and T_f, quantities are known for the chemical system, the entire kinetic event can be fully evaluated, with the assumption that there is no mechanism change taking place in the temperature range of interest.

In a zero-order or a quasi-zero-order (not far away from the initial temperature, T_0) case, the effect of ϕ is to slow down the reaction by a constant amount, i.e.

$$m_0 = \phi m_{0,s} \tag{26}$$

where $m_{0,s}$ is the experimentally determined initial rate for the entire system consisting of all the sample and the sample bomb.

Substituting eqn. (26) into eqn. (15), the TMR, θ_m, at temperature T_0 for the chemical system can be calculated from the experimental value, $\theta_{m,s}$ for the entire system, according to

$$\theta_m = \frac{\theta_{m,s}}{\phi} \tag{27}$$

providing eqn. (15) is a valid approximation.

RESULTS AND DISCUSSION

The principle discussed above is illustrated in a study of thermal decomposition of *N*-methyl-*N*-nitroso-*p*-toluene sulfonamide, commonly known as Diazald. The compound is a widely utilized reagent for the preparation of diazomethane, one of the most versatile reactants in organic synthesis. In the generation of diazomethane, Diazald is first dissolved in diethyl ether

before being allowed to react gradually with a basic solution. Diazald is known to be stable at room temperature. However, one instance has been reported where a sample stored for several months detonated spontaneously [24]; therefore, further understanding of its thermal kinetic property is highly desirable.

Kinetic modeling

As described in the experimental section, the ether solution of Diazald was subjected to a heat—wait—search operation in an ARC unit. A rate, 0.044°C min^{-1}, above the threshold, 0.02°C min^{-1}, set for the calorimeter unit was detected at 71.2°C and the calorimeter was maintained at an adiabatic condition until the completion of the reaction at 131.2°C.

Both the temperature and pressure recorded during the adiabatic reaction are shown in Fig. 6 as a function of reaction time. The expected vapor pressure of diethyl ether and the pressure of the gaseous products generated are also depicted in Fig. 6. A simple calculation without considering the gas solubility indicates that the amount of gas generated is about 0.4 mol mol^{-1} of starting material.

The temperature rate and the pressure rate vs. temperature plots are shown in Figs. 7 and 8, respectively. Shown in Fig. 9 is the plot of the pressure rate against the temperature rates on a log scale. A linear relationship

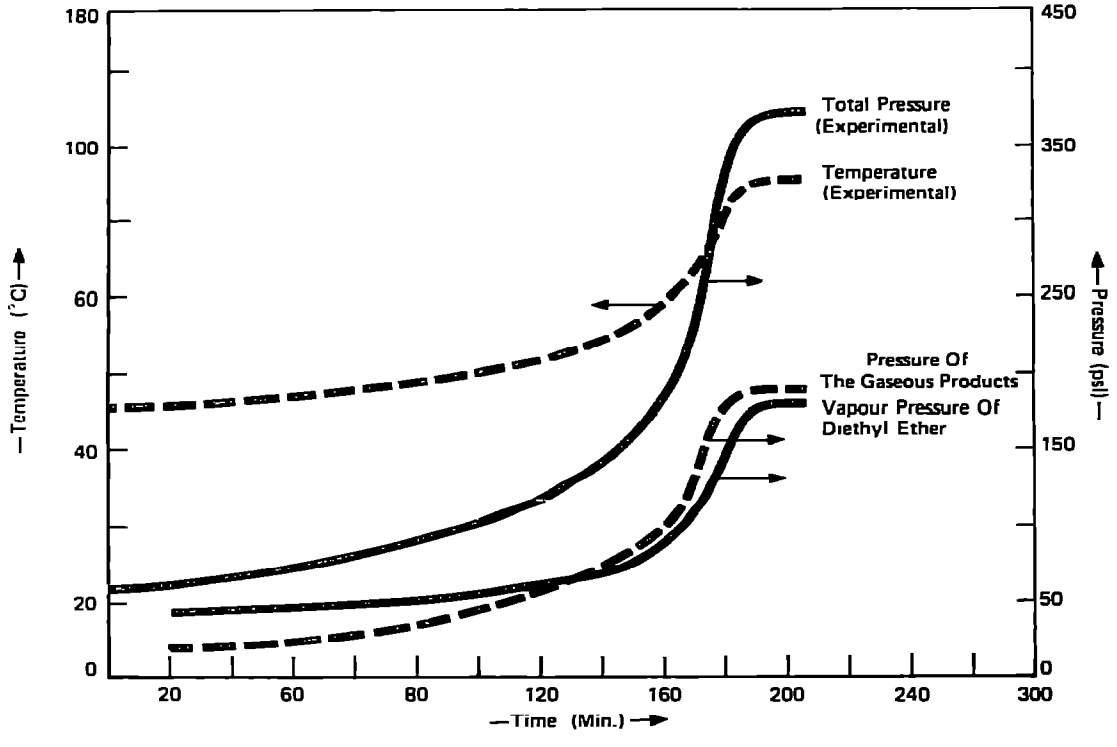

Fig. 6. The temperature and pressure vs. time curves of the thermal decomposition reaction of the Diazald®/diethyl ether solution.

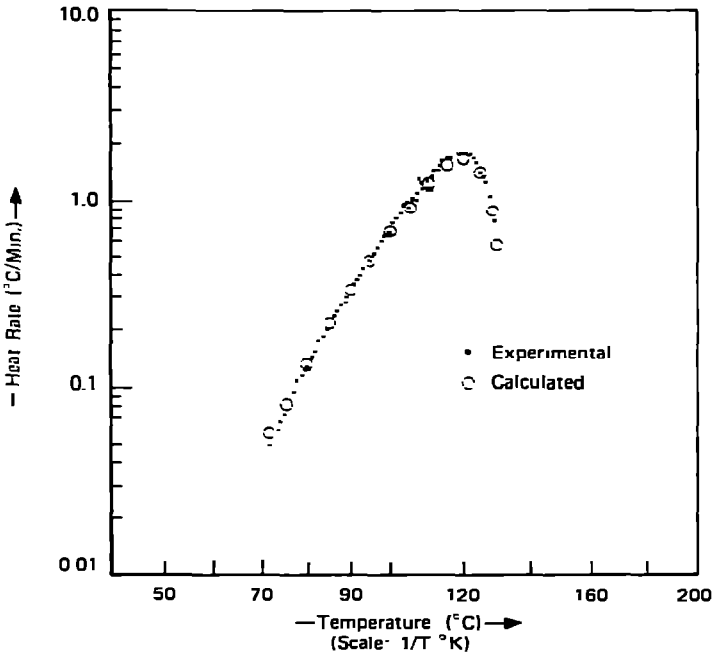

Fig. 7. The experimental and calculated self-heat rate vs. temperature curves of the thermal decomposition reaction of the Diazald®/diethyl ethyl solution.

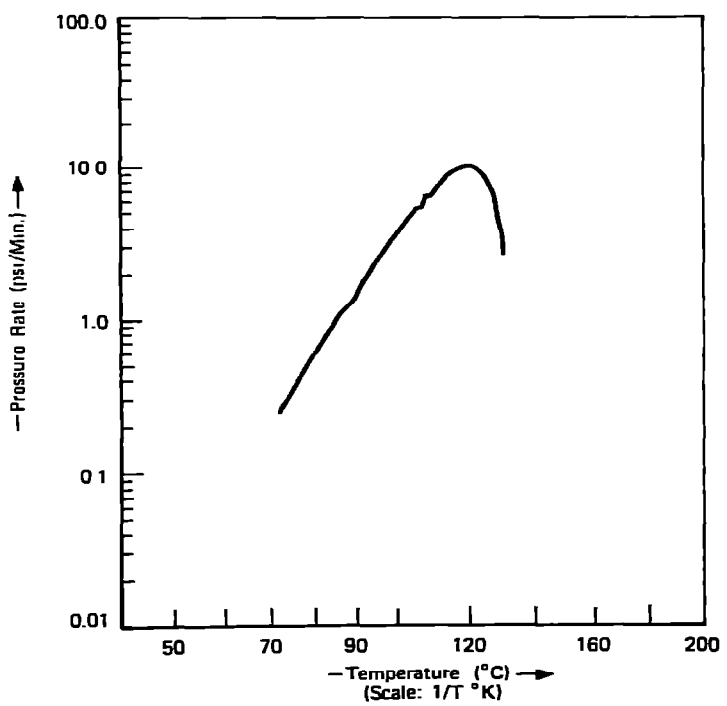

Fig. 8. The pressure rate vs. temperature curve of the thermal decomposition reaction of the Diazald®/diethyl ether solution.

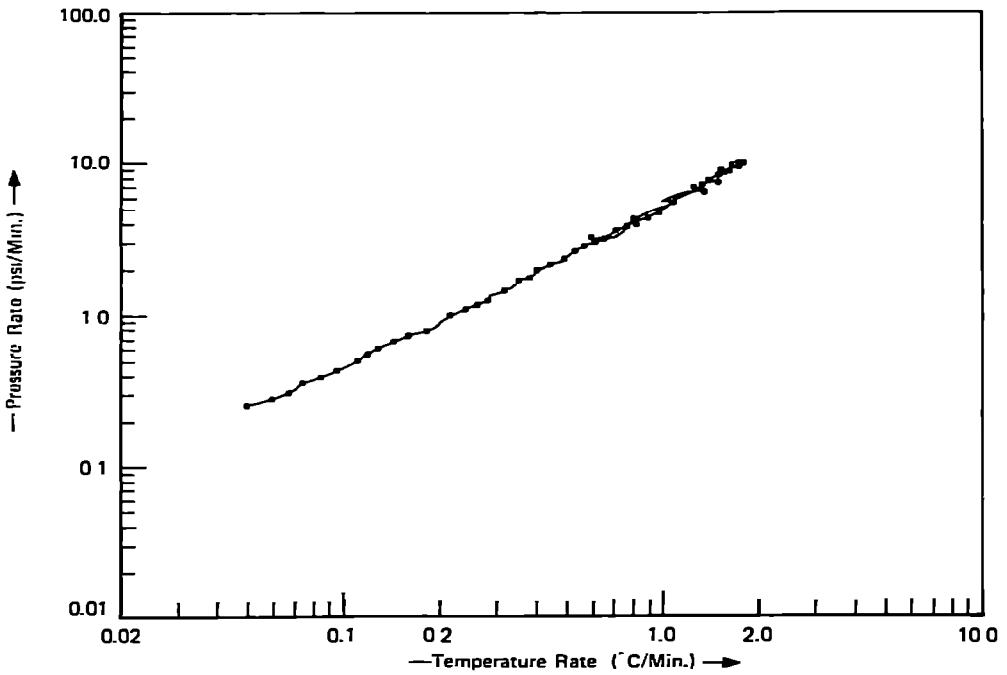

Fig. 9. The pressure rate vs. temperature rate curve of the thermal decomposition reaction of the Diazald®/diethyl ether solution.

was obtained. This is expected from examination of Fig. 6 in which both the pressure from the solvent and the gaseous product(s), and the temperature of the reaction system are similar exponential functions of the reaction time. The experimental data and the calculated results are summarized in Table 2.

TABLE 2

Experimental and calculated kinetic data of the Diazald/diethyl ether solution

	Exptl.	Calcd.	
Thermal inertia	2.0	2.0	1.0
Initial temperature (°C)	71.2	71.2	71.2
Final temperature (°C)	131.2	131.2	191.2
Adiabatic temperature rise (°C)	60	60	120
Initial self-heat rate (°C min^{-1})	0.044	0.057	0.114
Maximum self-heat rate (°C min^{-1})	1.8	1.7	190
Temperature at maximum rate (°C)	120	120	177.2
Time to maximum rate (min)	199	191 *	87 *
		143 **	74 **
Activation energy (kcal mol^{-1})		27.860	
Frequency factor (min^{-1})		4.58×10^{14}	
Heat of reaction of Diazald (kcal mol^{-1}) assuming C_v = 0.5 cal °C-g^{-1}		50	

* Numerical integration.
** Eqn. (14).

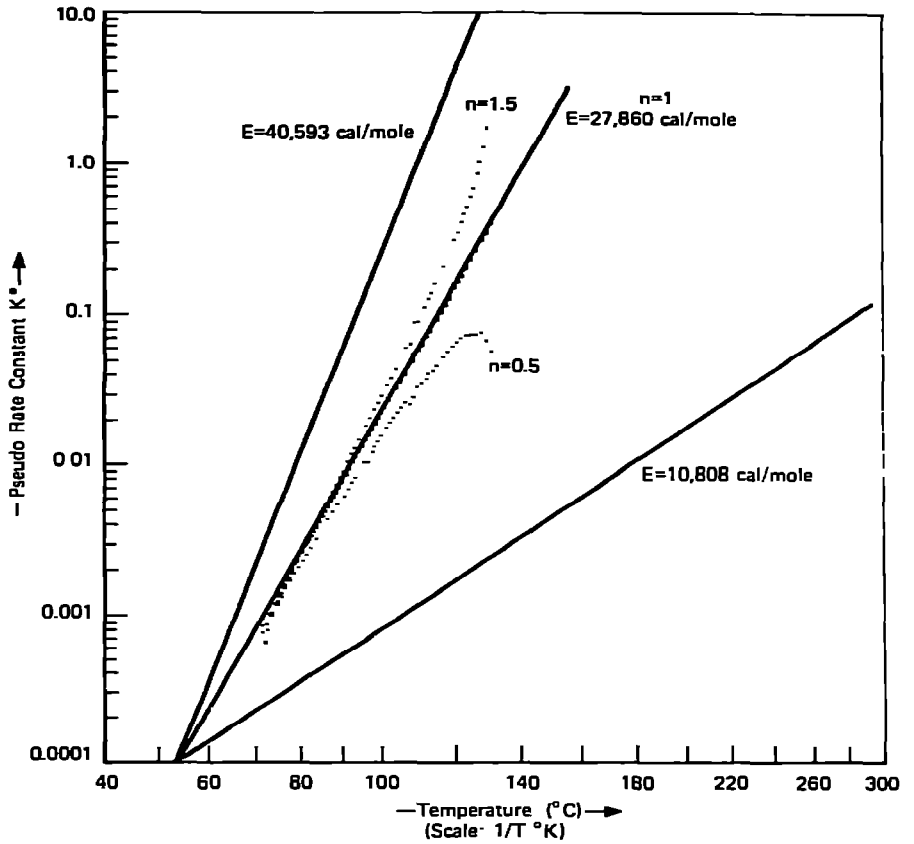

Fig. 10. The pseudo-order rate constant, k^*, vs. temperature curves of the thermal decomposition reaction of the Diazald®/diethyl ether solution and the two other model reactions.

Normally, the average heat capacity, $\overline{C}_v$, of the reactant is assumed to be 0.5 cal °C-g^{-1}; the heat of reaction is estimated according to eqns. (4) and (24) to be 230 cal g^{-1}. This gives the molar heat of decomposition of Diazald to be 50 kcal mol^{-1} as compared to 48 ± 7 kcal mol^{-1} by differential scanning calorimeter with the use of a modified glass ampule method [13].

Utilizing eqns. (6a) and (6b), the calculated pseudo zero-order rate constants, k^*, are plotted in Fig. 10 for three assumed reaction orders, n = 0.5, 1.0, and 1.5. The straight line in the case of n = 1 indicates that the reaction is first order. The Arrhenius kinetic parameters, E and A, are calculated to be 27.860 kcal mol^{-1} and 4.58 × 10^{14} min^{-1}, respectively. These values are used in the following calculations.

The calculated self-heat rate curve according to eqn. (5) for the reaction system is plotted in Fig. 7, along with the experimental curve included for comparison. The calculated quantities summarized in Table 2 are in good agreement with the experimental data, revealing that the kinetic parameters are quite reliable in describing the reaction in the temperature range of the experiment.

The calculated effect of thermal inertia on the self-heat rate and time—

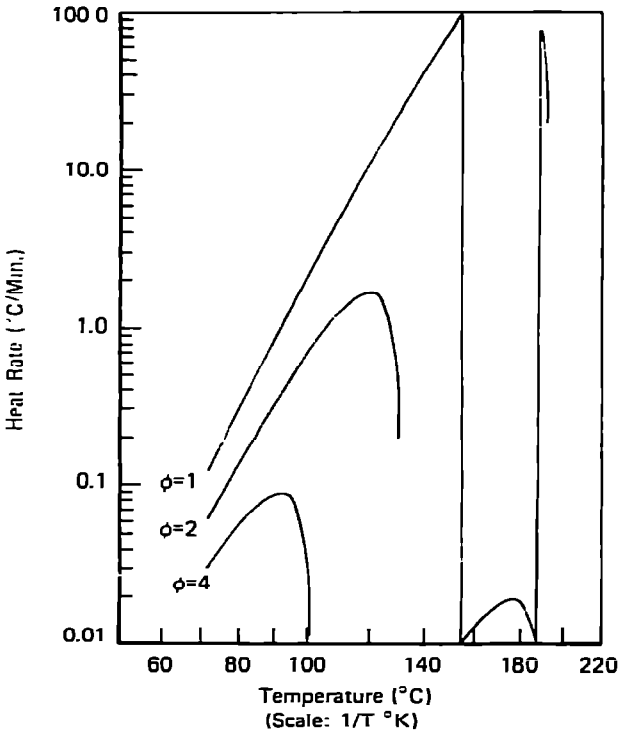

Fig. 11. The calculated effect of thermal inertia, ϕ, on the self-heat rates of the thermal decomposition reaction of the Diazald®/diethyl ether solution.

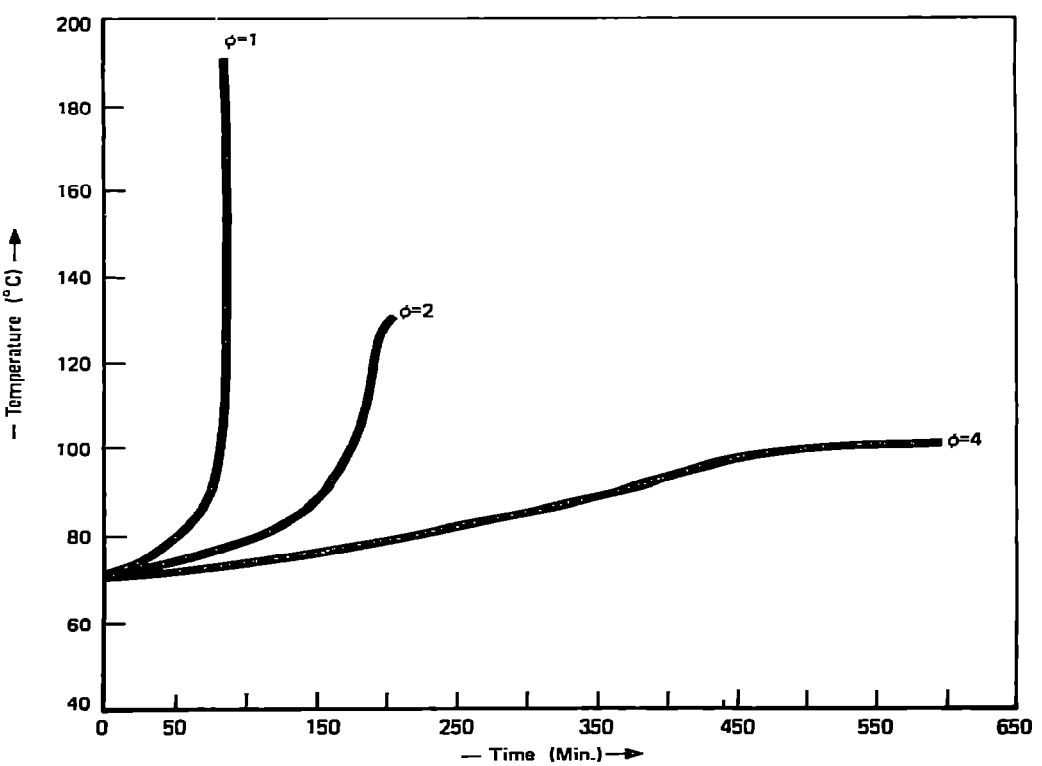

Fig. 12. The calculated effect of thermal inertia, ϕ, on the temperature and the reaction time of the thermal decomposition reaction of the Diazald®/diethyl ether solution.

temperature relationship are demonstrated in Figs. 11 and 12. A partial summary of the values is also presented in Table 2. It is obvious that the thermal inertia has a dramatic effect on the value of the maximum self-heat rate, and because of this effect, care must be taken when interpreting such data from an experiment with $\phi > 1$.

The effect on the initial rate for an adiabatic reaction is described in eqn. (26). A general expression in describing this effect over the entire experimental temperature range can be written

$$m_T = \phi\left[\frac{T_{0,s} + \phi\Delta T_{AB,s} - T}{\phi(T_{f,s} - T)}\right]^n m_{T,s} \tag{28}$$

The ratios, $m_T/m_{T,s}$, are calculated for some hypothetical cases with the same initial and final temperatures as those in the case of this study, but under different thermal inertia (ϕ) conditions, and the results are shown in Fig. 13. It is obvious that the lower thermal inertia, the less divergent are the

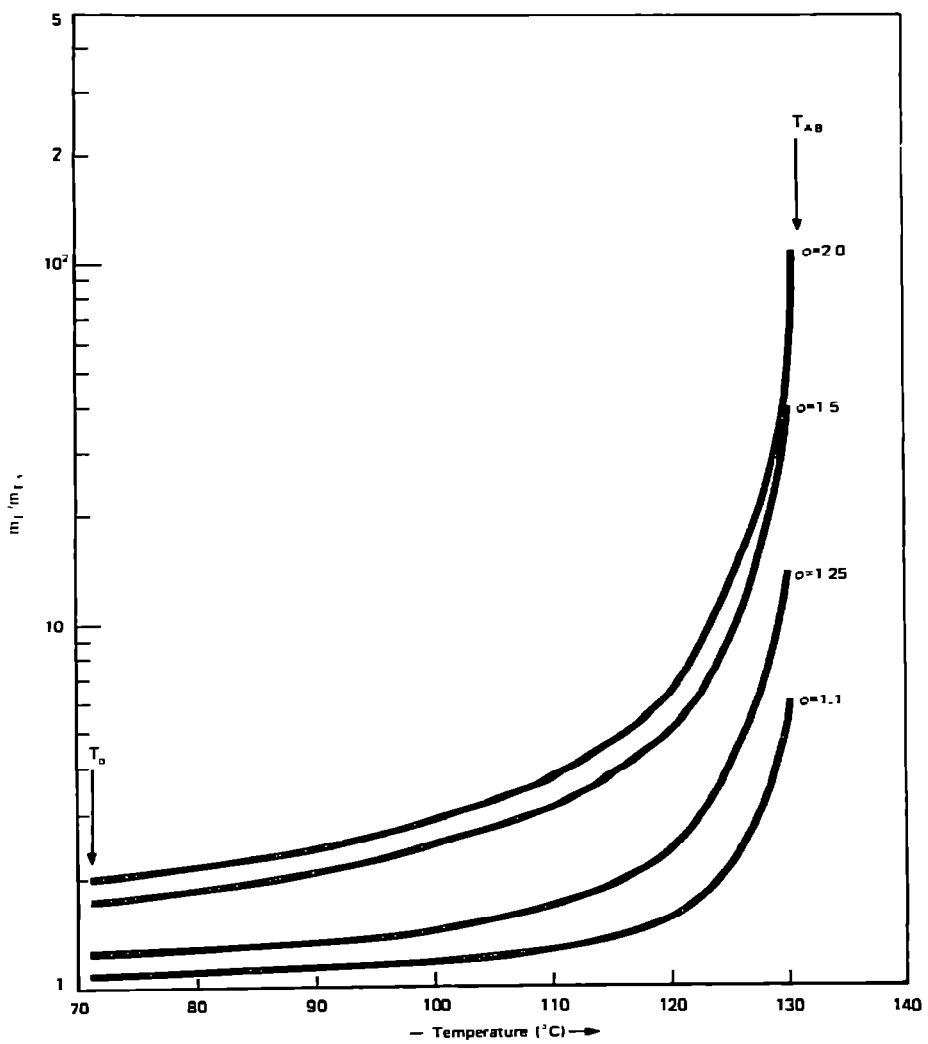

Fig. 13. The calculated effect of thermal inertia, ϕ, on $\theta_m/\theta_{m,s}$ for the thermal decomposition reaction of the Diazald®/diethyl ether solution.

ratios from being a constant in a wider temperature range. As indicated in eqn. (28), the ratios are not dependent upon the kinetic parameters, A and E, in the experimental range.

Based on the conservation of energy and the pseudo zero-order constants expressed in eqn. (7a), the following equation is derived in relating the initial temperatures under different thermal inertia conditions for a reaction with the same initial self-heat rate

$$\frac{1}{T_{02}} = \frac{1}{T_{01}} + \frac{R}{E} \ln \frac{\phi_1}{\phi_2} \tag{29}$$

where T_{02} and T_{01} are the initial temperatures under the thermal inertias ϕ_1, and ϕ_2, respectively, for the reaction with an activation energy E.

When it is applied to our present case, the initial temperature of the chemical system, $\phi_2 = 1$, with the same initial self-heat rate, 0.044°C min^{-1}, as determined in the experiment with $\phi_1 = 2$, is calculated to be 65.4°C, which is about 5.8°C lower than the experimental initial temperature of 71.2°C.

Accuracy of the analytical solution for θ_m

As discussed previously, the TMR, θ_m, has its significance in engineering design for determining the temperature of no return, T_{NR}, and reflects response time in a runaway situation. There are two ways of obtaining such information. One is through numerical integration as shown in eqn. (11); the other is through the analytical solution as proposed in eqn. (14). The accuracy of this equation is tested with the case presently studied and two arbitrarily chosen reactions with activation energies 40.593 kcal mol^{-1} and 10.808 kcal mol^{-1}, and frequency factors 1.44×10^{23} min^{-1} and 1.70×10^{3} min^{-1}, respectively. The pseudo rate constant, k^*, curves for the two chosen models are also shown in Fig. 10.

The calculated TMR curves based on numerical integration and analytical solution with and without the second term, $RT_m^2/m_m E$, retained in the expression are shown in Fig. 14, along with the experimental curves. Again, the excellent agreement between the numerically integrated and experimental curves supports the validity of the kinetic parameter obtained. The same calculations were carried out on the three model reactions under different thermal inertia conditions and the results are plotted in Figs. 15—17.

The first and second terms in the analytical solution for each case at the initial temperatures are summarized in Table 3. By examination of Figs. 15—17 and Table 3, the following conclusions can be drawn.

(1) The lower the activation energy, the more significant is the second term as compared to the first term in the analytical solution and the more divergent is the calculated value based upon the analytical solution from the true. The calculated TMRs based on the analytical solution without the second term are closer to those from the numerical integration near the initial temperatures.

(2) The higher the thermal inertia, the greater is the deviation between the numerical integration and the analytical solution.

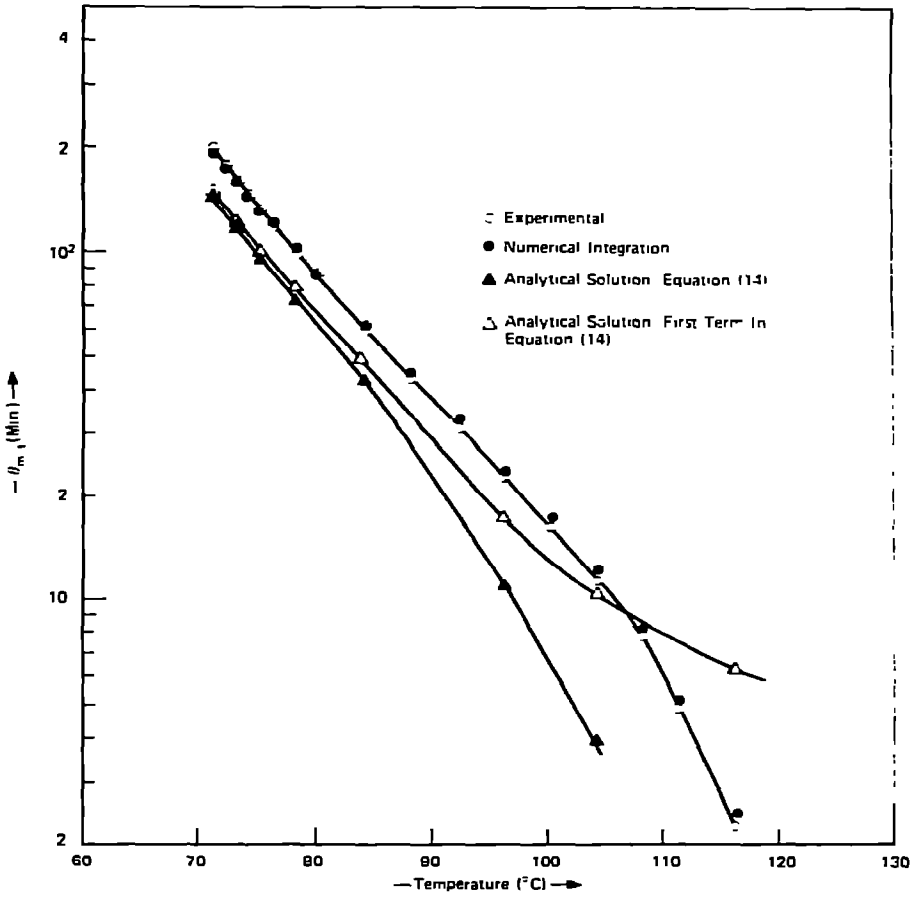

Fig. 14. Comparison of the calculated $\theta_{m,s}$ with the experimental $\theta_{m,s}$ for the thermal decomposition reaction of the Diazald®/diethyl ether solution.

(3) For a reaction with high activation energy, as in the case presently studied, the analytical solution is of a reasonable accuracy in estimating the TMR as might be required for engineering design.

Effect of initial temperature

The effect of initial temperatures on the self-heat rate and the times, TMR, are evaluated for the reaction studied, and the two reactions and the

TABLE 3

The calculated θ_{m_0} (min) for three model reactions at different thermal inertia conditions

E (kcal mol^{-1})	40.593		27.860		10.808	
ϕ	1	2	1	2	1	2
Analytical solution						
1st Term	49	99	74	150	230	460
2nd Tern	4.0×10^{-4}	0.32	0.074	6.60	82	370
Numerical integration	54	120	86	190	320	420

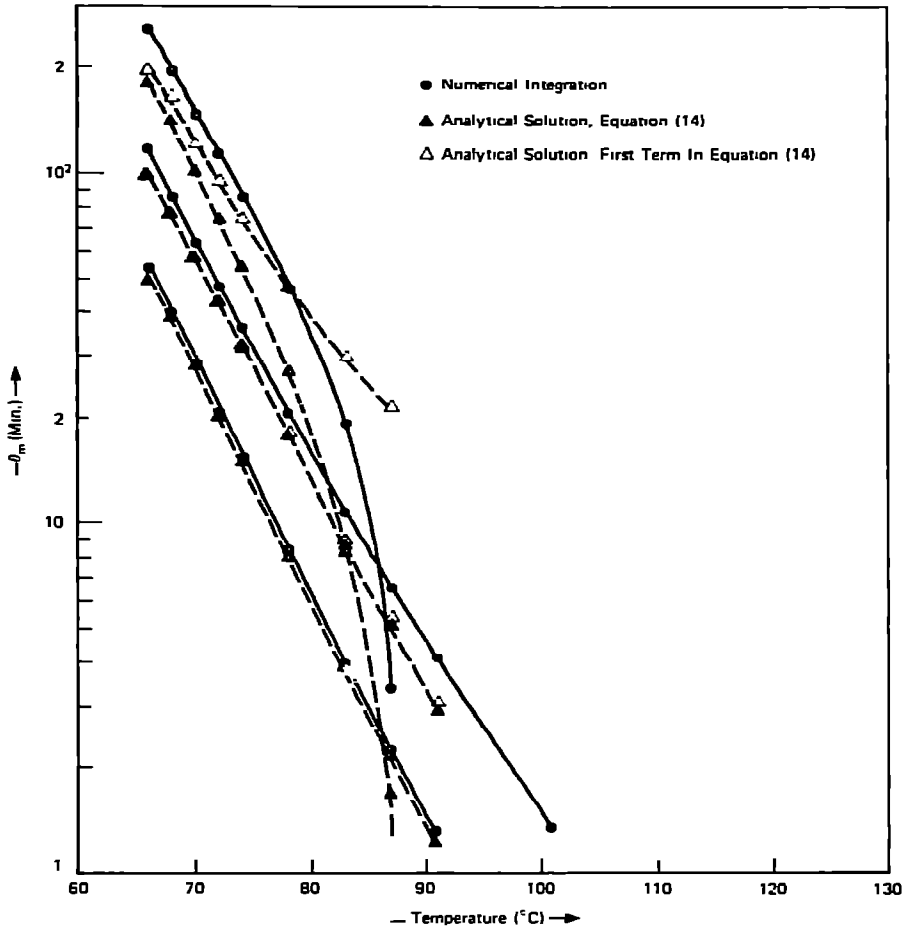

Fig. 15. Comparison of θ_m obtained from a numerical integration and the analytical solution for a model reaction with E = 40 593 cal mol^{-1} and A = 1.44 × 10^{23} min^{-1}.

results are shown in Figs. 18—20. The straight line formed by connecting the initial temperatures is the zero-order reaction line as described in eqns. (6a) and (27) with $T = T_0$. This line has a slope of E/R. The deviation of the zero-order TMR from a straight line [shown in Fig. 20(B)] is due to the inaccuracy of the analytical solution. The initial self-heat rate, m_0, is related to k^* by the equation

$$m_0 = \Delta T_{AB} k^*_{T_0}$$

obtained from a combination of eqns. (6a) and (7a).

As discussed previously, when the initial temperature increases, the initial rate increases following the zero-order line. At a temperature T^*, the reaction decelerates, even though the temperature itself continues to rise. The value of T^* can be evaluated with eqn. (10) to be 834, 644, and 298°C for the three model reactions, providing no mechanistic changes occur in the temperature range under consideration.

The trend in reaching T^* is clearly shown in Fig. 20(A). Theoretically,

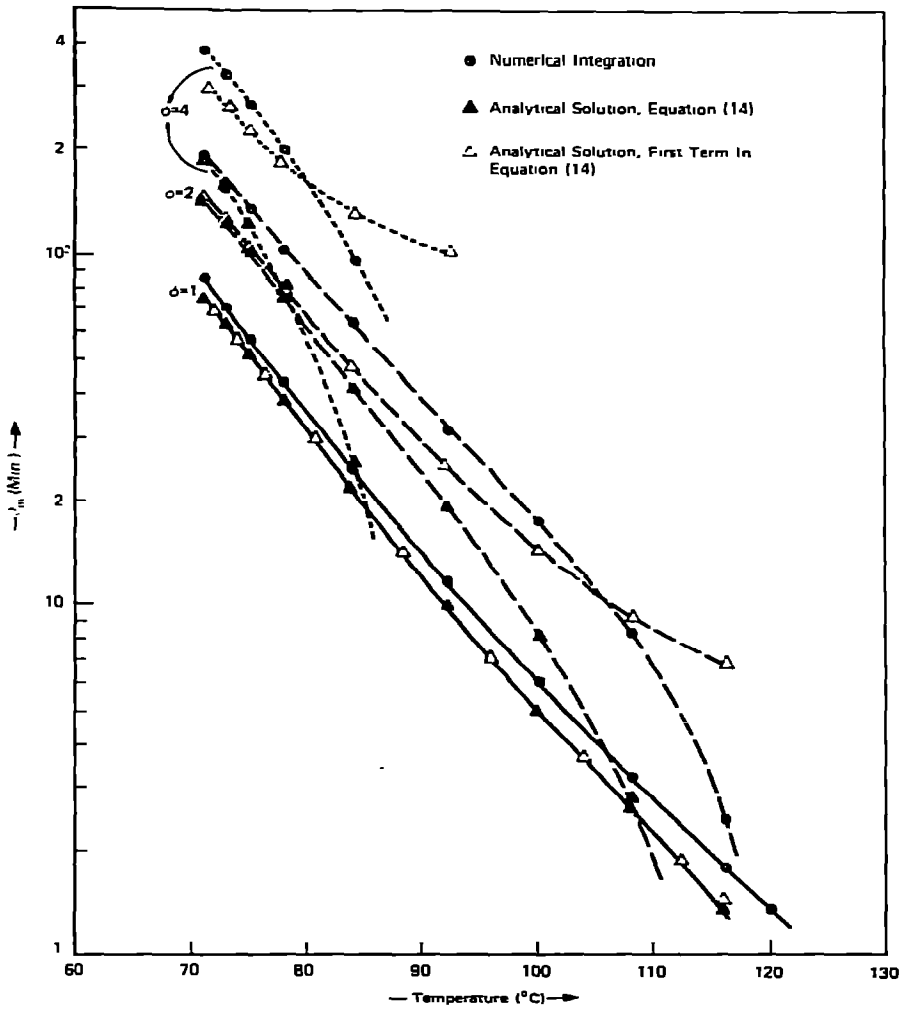

Fig. 16. Comparison of θ_m obtained from a numerical integration and the analytical solution for the thermal decomposition reaction of the Diazald®/diethyl ether solution with E = 27 860 cal mol^{-1} and $A = 4.58 \times 10^{14}$ min^{-1}.

each reaction does exhibit its own T^*, As shown in eqn. (10), T^* also depends upon the adiabatic temperature rise, $\Delta T_{AB,s}$. The higher the thermal inertia, the lower is $\Delta T_{AB,s}$ and T^*.

Calculation of T_{NR}

Generally speaking, two major aspects can be evaluated from the results obtained in a thermokinetic study. One is the quality point of view, while the other is hazard determination. In hazard evaluation, the fundamental question is to define a set of operating conditions at which a runaway reaction cannot occur. As discussed previously, a thermal runaway reaction does not necessarily lead to an explosion. However, if the reaction is associated with a release of gaseous products, a pressure increase will naturally result. An

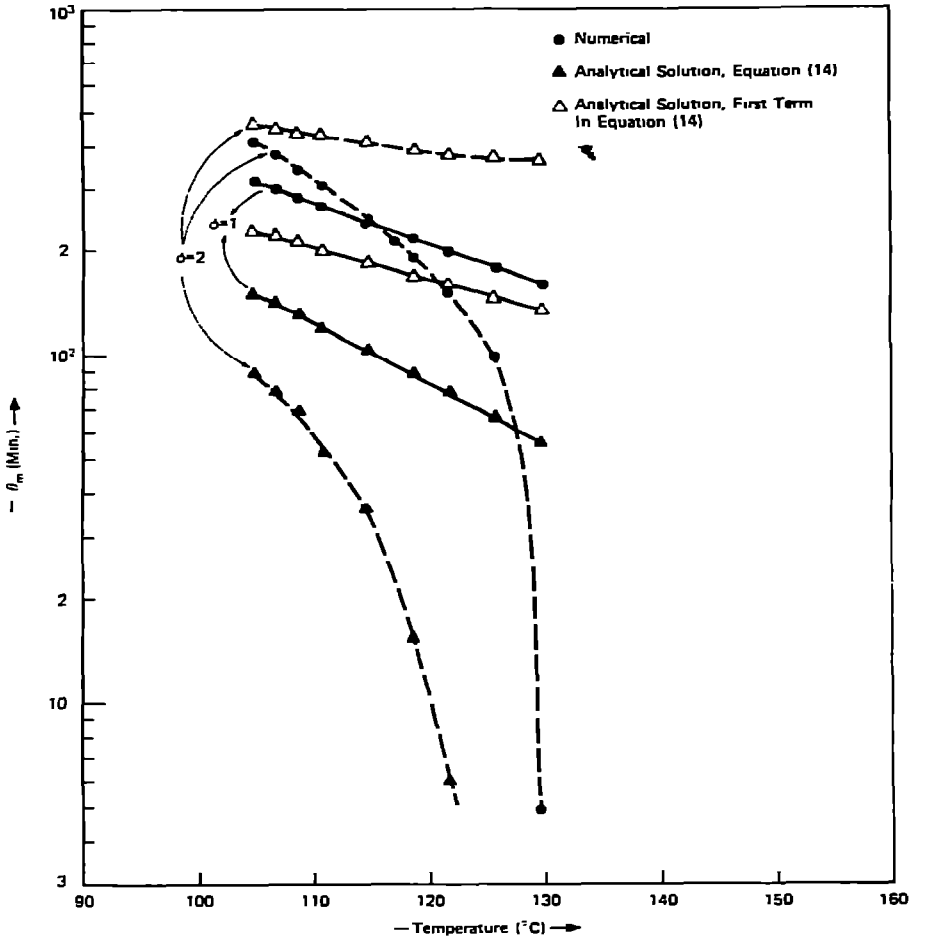

Fig. 17. Comparison of θ_m obtained from a numerical integration and the analytical solution for a model reaction with E = 10 808 cal mol^{-1} and $A = 1.70 \times 10^3$ min^{-1}.

explosion is conceivable once the pressure from the gaseous products exceeds the vessel strength.

The temperature of no return, T_{NR}, is one of the safety parameters which can be determined by the present technique. Knowledge of the heat transfer property of a vessel or equipment time line, MC_v/Ua, is required before the determination of T_{NR} is possible. The equipment time line can be determined experimentally from the slope of the time—temperature cool-off curve of the equipment initially filled with a fluid at an elevated temperature or estimated from an experienced runaway reaction in an equipment. The equipment time line of a standard 500 ml three-neck flask two-thirds full of organic material was determined as ~20 min, and that of a 10 000 gal well-insulated tank car was estimated to be 23 days.

Figure 21 shows the experimental TMR, $\theta_{m,s}$, with $\phi = 2$, the derived TMR, θ_m and the zero-order TMR, θ_{m_0} curves of the diethyl ether solution of Diazald. The zero-order TMR curve for pure Diazald was also calculated from the kinetic and thermodynamic data obtained by considering the sol-

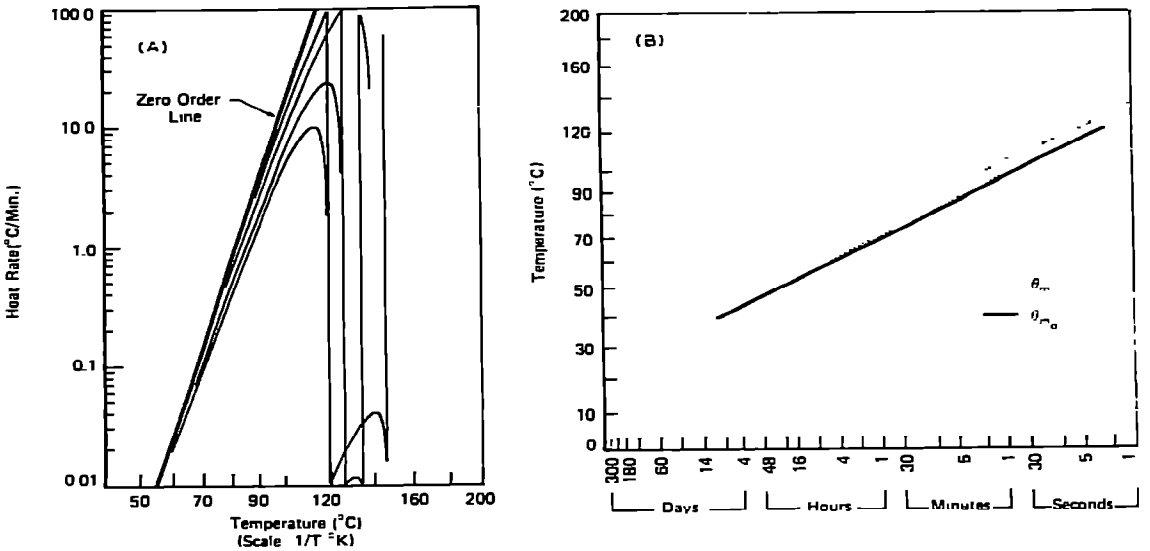

Fig. 18. The calculated effects of initial temperatures on the self-heat rates (A) and times to maximum rate (B) for a model reaction with E = 40 593 cal mol^{-1} and A = 1 44 X 10^{23} min^{-1}.

vent as being part of the bomb. With this consideration, thermal inertia is estimated to be 7.6, assuming the average heat capacities of diethyl ether and Diazald in solution to be 0.5 cal °C-g^{-1}. Naturally, an assumption, without proven evidence, has to be made that the kinetic event taking place in the

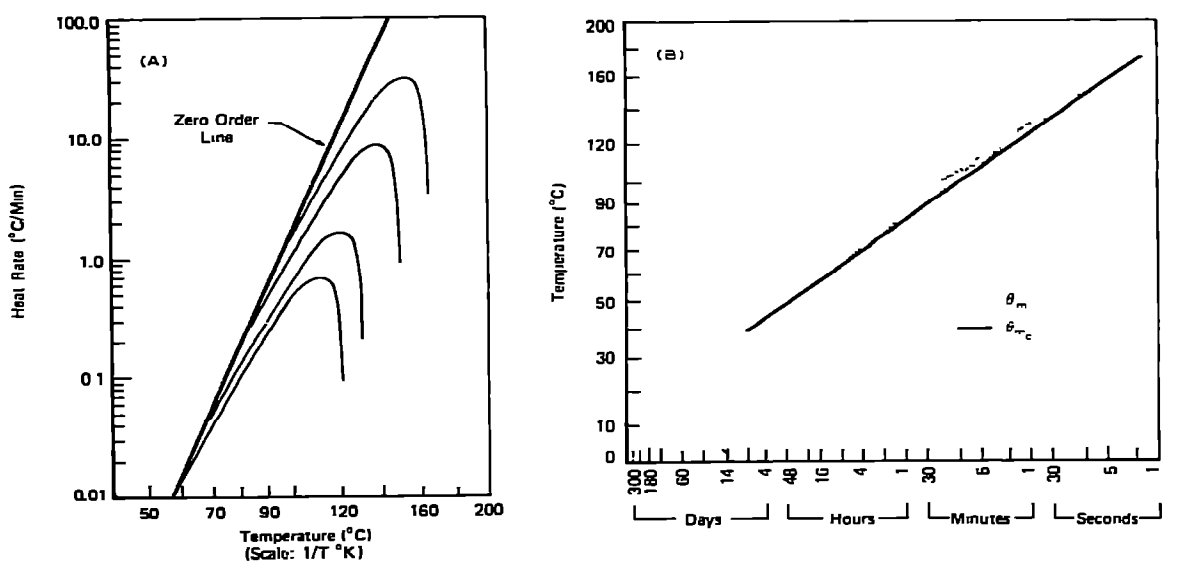

Fig. 19. The calculated effects of initial temperatures on the self-heat rates (A) and times to maximum rates (B) for the thermal decomposition reaction of the Diazald®/diethyl ether solution with E = 27 860 cal mol^{-1} and A = 4.58 x 10^{14} min^{-1}.

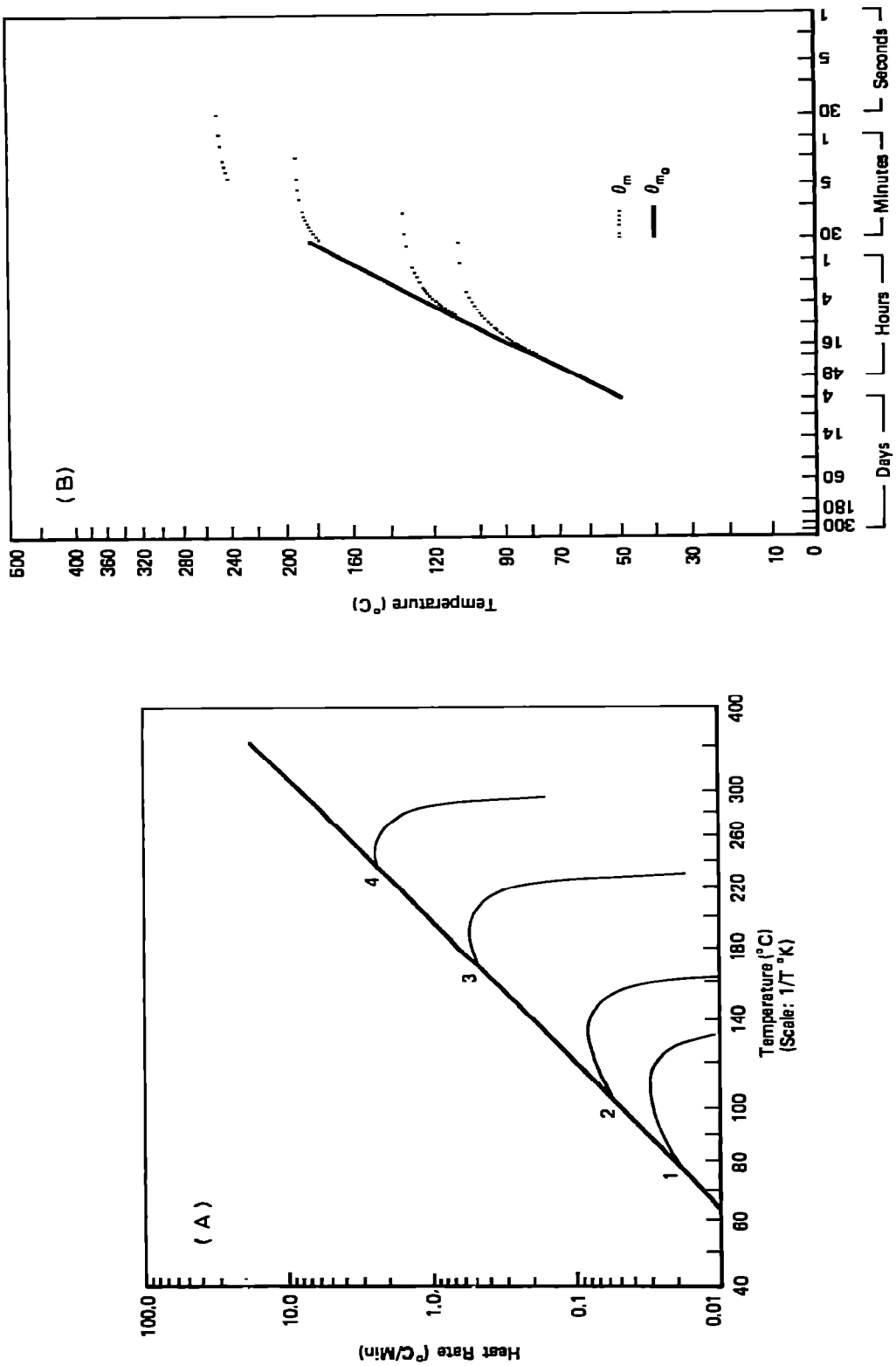

Fig. 20. The calculated effects of initial temperatures on the self-heat rates (A) and times to maximum rates (B) for a model reaction with $E = 10\,808$ cal mol^{-1} and $A = 1.70 \times 10^3$ min^{-1}.

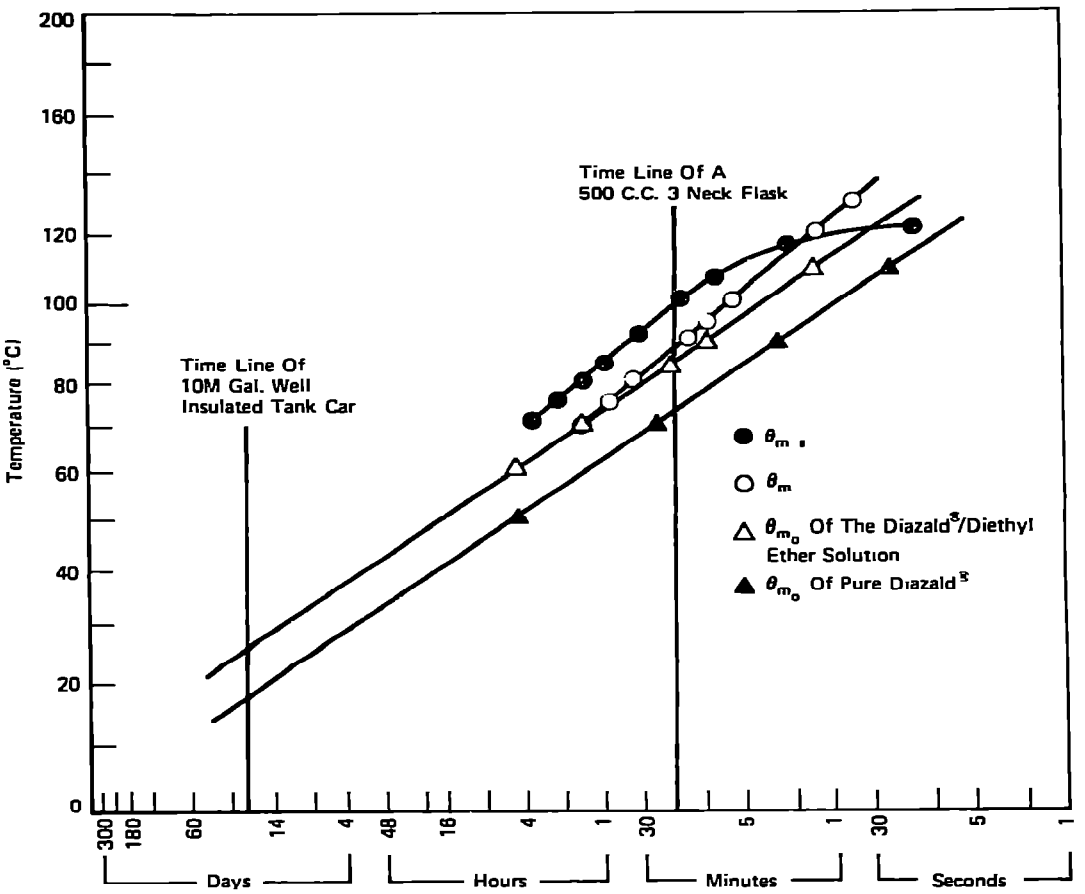

Fig. 21. Graphic determination of T_{NR} from the time-to-maximum-rate curves of the thermal decomposition reaction of Diazald® and the equipment time curve.

solid state is the same as that in the solution. Admittedly, risk may be involved in this assumption.

For the two vessels mentioned above, the equipment time lines are plotted in Fig. 21. This leads to the T_{NR} of the solution and pure Diazald to be ~73 and ~85°C, respectively, in the case of the standard 500 ml three-neck flask. From this study, handling or storing this solution or pure Diazald in laboratory vessels at ambient temperature does not present any thermal hazard. However, in the case of the 10 000 gal well-insulated tank car, the T_{NR}s, as shown in Fig. 21, are ~26 and 18°C for the solution and pure Diazald, respectively, assuming that one can extrapolate the kinetic data to lower temperatures. Under such conditions, a thermal runaway and a possible explosion due to the pressure build-up are predicted if the ambient temperature is higher than T_{NR}.

Complex reactions

It is recognized that most of chemical reactions encountered in the hazard study cannot be kinetically modeled because of their natural complexity.

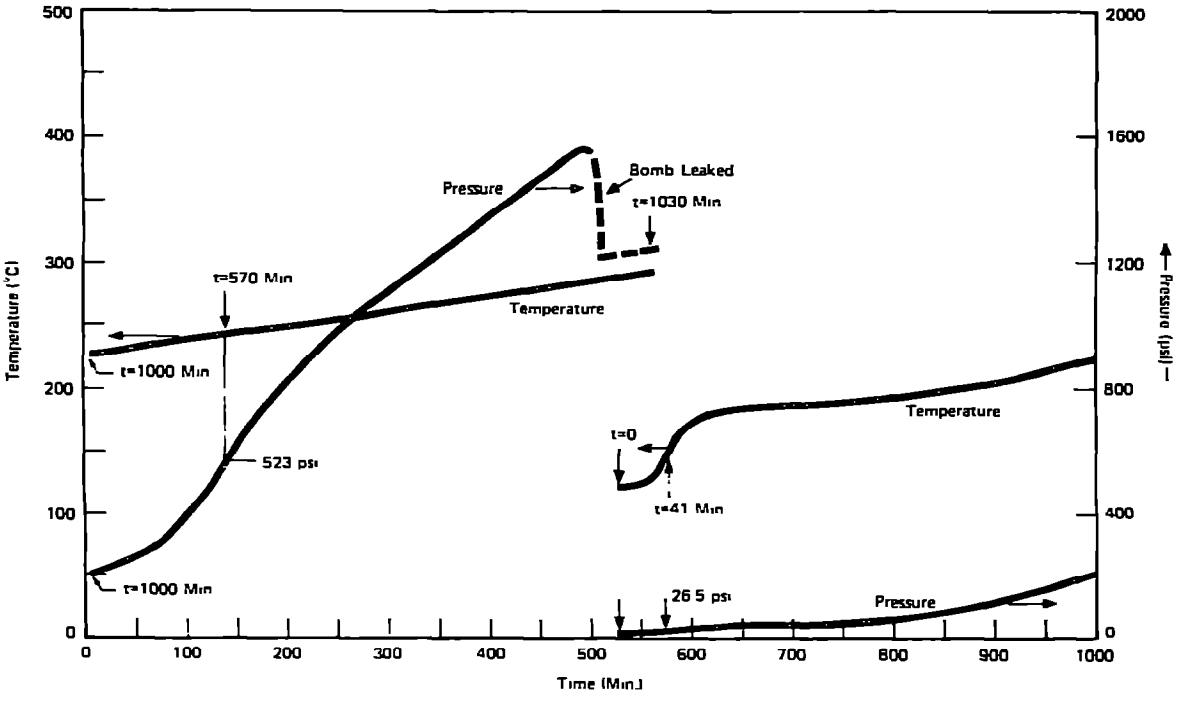

Fig. 22. The temperature and pressure vs. time curves of adiabatic reactions taking place in a monomer sample.

However, the accelerating rate calorimeter still shows its uniqueness in qualitative, if not quantitative, understanding of a thermokinetic event. An example now given demonstrates this powerful technique in a general hazard evaluation of a complex reaction.

As shown in Figs. 22 and 23, many exothermic reactions are taking place after the initial reaction which cause the temperature of the chemical system to continue to rise, but at much slower rates. A significant pressure rise was observed when the temperature reached ~200°C, at which time self-heat rate was only 0.18°C min^{-1}. The pressure rate increased 10-fold in magnitude, from ~0.4 psi min^{-1} to its maximum ~5 psi min^{-1} at 244°C, and the pressure continued to rise up to 1600 psi at ~285°C. An explosion could thus be caused by the latter exothermic reactions. In this case, the thermal hazard associated with the above reactions may not be as important as the explosion hazard.

It is conceivable that the first reactions may reflect a polymerization process. The heat resulting from this reaction can trigger the latter exothermic reactions under adiabatic conditions and cause the decomposition of the newly formed product with the generation of gaseous product(s). For further understanding of the chemistry, a chemical analysis of the product(s) after the completion of the ARC run is essential.

For the case described above, it is understandable that any detailed kinetic modeling would be out of reach. However, thermodynamic quantities, such as the heat of reaction and final pressure, can be easily evaluated quantita-

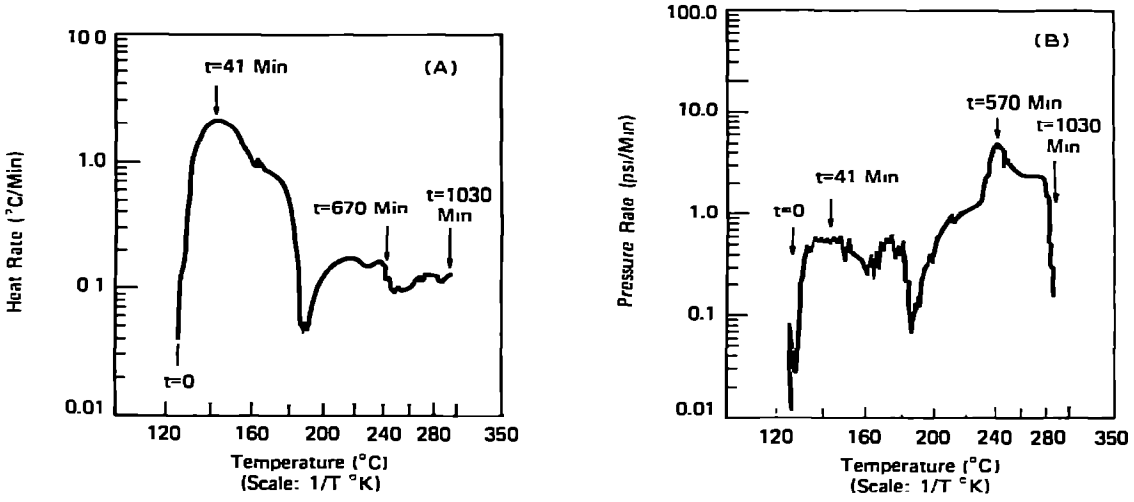

Fig. 23. The self-heat rate (A) and pressure rate (B) vs. temperature curves of adiabatic reactions taking place in a monomer sample.

tively, since they only depend upon the initial and final states of the chemical system, and not upon the kinetic routes to reach the final state.

CONCLUSION

As demonstrated in this paper, the accelerating rate calorimetric technique is unique in providing information concerning temperature and pressure of reactions taking place under adiabatic conditions. The information obtained is pertinent in hazard evaluation. For an *n*th-order reaction, mathematical modeling of a kinetic event is possible. The information obtained can be used for engineering considerations to prevent a runaway reaction. For complex reactions, the experimental data reflect the complexity of the mechanism, but the experiment can be run as a simulation by matching of the thermal inertia of the sample and bomb with the system of interest. If true adiabatic information relative to the chemicals is required, the extrapolation of the information obtained from the experiments carried out at several different thermal inertias are needed. Currently, the thermal inertias of the different sample bombs with half the volume being filled are in the range 1.2—4.5. Finally, when used as a preventative tool, only temperature and pressure data in the initial narrow temperature range are needed and limited extrapolation may be a valid and practical approach to the problem.

As in any other type of accelerating studies, such as studies in polymer weathering and aging, persistency of pollutants in the environment, etc., the extrapolation of the accelerating rate calorimetric data achieved in a short laboratory experiment to a much longer time, as required in cases of storage and transportation, is a required operation. Validation of this extrapolation is technically difficult before the event, and a retroactive validation after the undesirable runaway event is very possible.

Undoubtedly, the accelerating rate calorimetric technique introduced in this paper is in its incipient stage; much remains to be explored. Hopefully, increase in the availability of the technique through commercialization can promote a faster and progressive advance toward the understanding and utilization of the technique.

ACKNOWLEDGEMENTS

The authors would like to express their sincere gratitude to K. Pete, R. Solem, V. Caldecourt, G. Crable, E. Timm, and H. Kohlbrand, for their interest and effort in developing the technique described in this paper; also to J. Evans, H. Gill, and J. Kochanny for their careful review of this manuscript.

REFERENCES

1 A A. Duswalt, Thermochim. Acta, 8 (1974) 57 and the reference therein.
2 T. Ozawa, J. Therm. Anal., 2 (1970) 301.
3 ASTM Standard Method number pending.
4 C.J.H. Schouteten, S. Bakker, B. Klazema and A.J. Pennings, Anal. Chem., 49 (1977) 522.
5 W.W. Wendlandt, Anal. Chim. Acta, 49 (1970) 188.
6 H.W. Hoyer, A V. Santoro and E.J. Barrett, J. Polym. Sci. Part A-1, 6 (1968) 1033.
7 F.E. Freeberg and T.G. Alleman, Anal. Chem., 38 (1966) 1806.
8 K.E.J. Barrett and H.R. Thomas. J. Polym. Sci. Part A-1, 7 (1969) 2621.
9 V.W. Knappe, G. Nachtrab and G. Weber, Angew. Makromol. Chem., 18 (1971) 169.
10 K. Horie, I. Mitta and H. Kambe, J. Polym. Sci. Part A-1, 6 (1968) 2663.
11 G.R. Taylor, G.E. Dunn and W.B. Easterbrook, Anal. Chim. Acta, 53 (1971) 452.
12 J. Chiu, Thermochim. Acta, 26 (1978) 57.
13 J.C. Tou and L. Whiting, to be published.
14 J. Hakl, Eighth North American Thermal Analysis Society Conference, Atlanta, Georgia, Oct. 15—18, 1978
15 A.V. Zatka, Thermochim. Acta, 28 (1979) 7.
16 L. Walker, The Fifth International Conference on Chemical Thermodynamics, Aug. 1977, Ronneby, Sweden.
17 D.I. Towsend, Chem. Eng. Prog., 73 (1977) 80.
18 CSI—ARC Manuals, Columbia Scientific Industries, Austin, Texas.
19 K.T. Pate and R.H. Solem, to be published.
20 E. Ball, F. Rust and W. Vaughan, J. Am. Chem. Soc., 72 (1950) 337.
21 J. Murawski, J Roberts and M. Szward, J. Chem. Phys., 19 (1951) 698.
22 K. Hirota and I. Mirjashita, J. Chem. Phys., 18 (1950) 561.
23 J. Raley, F. Rust and W. Vaughan, J. Am. Chem. Soc., 70 (1948) 1336, 2767.
24 Technical Information, Product No. D2800-0, Aldrich Chemical Co. Inc., Sept. 1975.
25 O.M. Todes, Acta Physicochim. URSS, 5 (1936) 785.
26 S.H. Lin and H. Eyring, Ann. Rev. Phys. Chem., 21 (1970) 255.